RSC Advances

ROYAL SOCIETY OF CHEMISTRY

www.rsc.org/advances

Cite this: DOI:

www.rsc.org/

COMMUNICATION

Self-assembled synthesis and surface photovoltage property of polyhedron-constructed micrometer solid spheres and hollow-spheres In_2S_3

Yan Shi,[a] Yu-Lin Yang,*[a] Rui-Qing Fan, *[a] Liang Li,[a] Jia Yu[a] and Shuo Li[a]

Received (in XXX, XXX) Xth XXXXXXXXX 200X, Accepted Xth XXXXXXXXX 200X

DOI:

β-In_2S_3 solid micro-spheres composed of wedge-like octahedra, and hollow micro-spheres composed of nanorods have been fabricated by a simple one-step hydrothermal treatment. The unique surface photovoltage property of as-prepared In_2S_3 samples were investigated through surface photovoltage (SPV) spectroscopy.

Nowadays, the controllable synthesis of micro- and nano-scale materials with unique morphology has attracted intensive interest due to their significance in basic scientific research and technology applications.[1] Several researchers have synthesized and characterized varied morphology of metal oxides or chalcogenides. Studies have focused on functional metal chalcogenides/oxides materials with special micro- or nano-scale morphologie, such as two-dimensional monolayer MoS_2,[2] hollow/solid Ag_2S/Ag heterodimers as antibacterial,[3] floral Ga_2O_3 nanorods as pholocatalyst[4] and hollow spherical TiO_2 for dye-sensitized solar cells.[5]

As a III–VI chalcogenide and n-type semiconductor material, In_2S_3, has potential special optical, photo-conductive and electronic properties because of its defected spinel structure.[6] In_2S_3, a band gap of 2.0 ~ 2.3 eV[7] responding to visible light, is a potential photoelectrical substitute for the highly toxic CdS as a buffer layer in $CuInSe_2$ and $CuInS_2$ based solar cells to reduce toxicity.[8] In_2S_3 nano- or micro-material has a promising future in many fields. So far, many physical and chemical methods such as vapor–liquid–solid growth,[9] chemical vapor deposition,[10] solvothermal[11] and wet chemical synthesis with various templates or without[12] have been devoted to the synthesis of varied In_2S_3, most of them are single monolithic structure such as nanoflakes,[13] nanowires,[14] nanotubes,[15] nanobelts,[11] hollow microspheres[16] and nanorods.[10] Nano/micro-sized In_2S_3 with composite structure can be rarely found in literatures. Recently, preparations of hollow nano/micro-particles structures by a simple template method with some interesting physical phenomena have been demonstrated.[17] This communication presents a simple one-step hydrothermal synthesis of solid micro-spheres composed of wedge-like octahedra. And hollow micro-spheres β-In_2S_3 composed of one-dimensional (1D) nanorods are synthesized with sodium dodecyl sulfate (SDS) as the template. This is the first time studied surface photovoltage property about In_2S_3 powders.

In a typical procedure, 1.0 mmol indium chloride (the reaction product of elemental indium and hydrochloric acid) and 1.5 mmol thiourea were added to 30.0 mL deionized water in a 50 mL Teflon-lined stainless steel autoclave and stirred for 30min. After the autoclave was sealed and maintained at 165 °C for 24 h in a preheated oven and cooled to room temperature naturally. Repeatedly centrifugation and washed with absolute ethanol and distilled water, then volatilized naturally in the ventilation at room tempreture. Red powder was obtained as sample **1**. The procedure of coordination sample **2** was similar to the sample **1** except 0.35 mmol SDS was added in the raw material. The transparent solution was obtained, and then heated at 165 °C for 24 hours. Red products were collected after treatment.

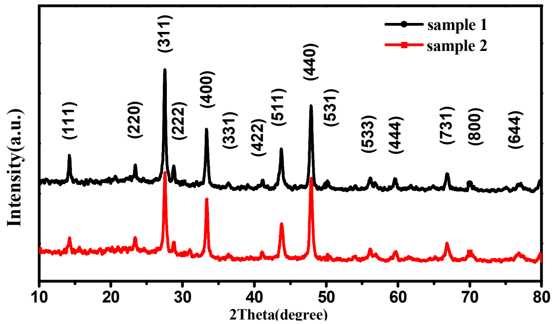

Fig. 1 XRD patterns of In_2S_3 samples.

X-ray diffraction (XRD) was used to investigate the crystalline structure of the as-prepared In_2S_3 (Fig. 1). All the reflections could be indexed to β-In_2S_3 (JCPDS No.65-0459). No characteristic peaks were observed for the other impurities such as In_2O_3, InS and $In(OH)_3$. It shows that in all the samples main characteristic peaks are observed at 27.4°(311), 33.2°(400), 43.6°(511) and 47.7°(440). According to the Scherrer equation,[18] the average crystallite sizes of sample **1** and **2** are *ca*. 25 nm and 22 nm.

The typical scanning electronic microscopy (SEM) images of β-In_2S_3 samples are presented in Fig. 2. Inside, Fig. 2a-2c showed SEM pictures of the sample **1**. From Fig. 2a, the morphology of sample **1** is uniform solid-spheres. The particle's diameter is about 9 μm which belong to solid micro-spheres, and the solid spheres are composed of many tiny particles of polyhedron packing together densely (Fig. 2b). Furthermore, from Fig. 2c these tiny polyhedral particles on the spheres are similar to octahedron, except the vertex of octahedron grows into the arris, as four faces of octahedron have four edges, and other faces have three edges. Compared with other researches,[19] not only the diameter of sample **1** is longer, but also the mutation of octahedron structure unit is different from typical octahedron, and this octahedron structure unit tends to be wedge-like.[20] And the size of this construction unit is length (*ca*. 750 nm), width (*ca*. 600 nm) and height (*ca*. 800 nm). SEM pictures of the sample **2**

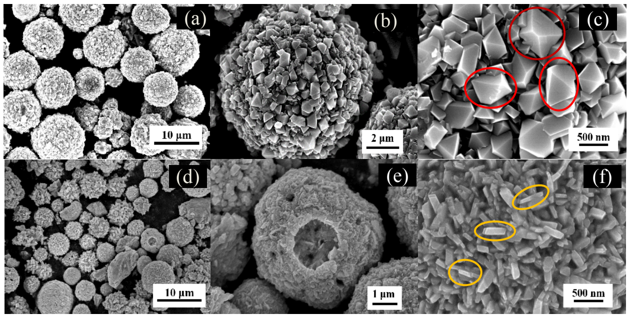

Fig. 2 SEM images of (a-c) sample **1** (solid-spheres) from low to high magnification; (d-f) porous hollow-spheres In_2S_3 particles (sample **2**) with from different magnifications.

showed in Fig. 2d-2f. The average size of these micro-spheres with many holes on the surface is about 6 μm smaller than sample **1** (solid-spheres) (Fig. 2d). The enlarged drawing of hollow-spheres displays that these spheres with many holes are hollow-spheres (Fig. 2e). Apparently, the particles form hollow-spheres are parallelepiped with the length about 350 nm, the height about 100 nm and the thickness about 50 nm (Fig. 2f). Therefore, tiny nanocrystals are 1D nanorods. In some sense, In_2S_3 hollow-spheres samples are composed of nanocrystals. On the basis of Fig. 2, sample **2** has smaller size than sample **1**.

In the aqueous solution, ionization of $InCl_3$ generates In^{3+} ions. It is generally believed that metal ions can coordinate with thiourea in aqueous solution to form metal-thiourea compound.[21] A possible reaction mechanism is shown in Scheme 1. Free In^{3+} ions combine thiourea to form $[In(SC(NH_2)_2)_n]^{3+}$ complexes, which will decompose into In_2S_3 nuclei under the hydrothermal condition. To decrease the total surface free energy under the constraint of fixed volume, tiny In_2S_3 nucleis are grow up to formed polyhedral shape. Once the reactant ions were depleted, crystal dissolution might occur at the high-energy surfaces, and driven by the minimization of the total energy of the system. Tiny In_2S_3 particles can be self-assembled into microspheres, which can be due to aggregation-based mechanism under hydrothermal conditions.[19] The formation of In_2S_3 hollow micro-spheres can be attributed to the SDS generated a core-shell type that the negative charge $R\text{-}SO_4^-$ come from SDS molecule was outside during the hydrothermal process. SDS, an anion surfactant, often acts as a template during synthesis of various sulfides/oxides.[22] Those negative charges attracted $[In(Thiourea)_n]^{3+}$ complex that were carried from water to the interface of SDS-water. Attributed to the interreaction between $R\text{-}SO_4^-$ anion and $[In(Thiourea)_n]^{3+}$ complex, react condition of reflux may have led to the formation of sheet-like micelles of SDS as anionic template. And SDS makes nanoparticles grow along these templates which serves as the nuclei for the nanoparticles growth as nanorod-like with a hexahedral shape. With the hydrothermal carrying out, the common result of both tiny In_2S_3 particles self-assembly and the group of SDS composed particle might be formation of hollow microspheres. With SDS removed, hollow-spheres In_2S_3 are formed with many holes.

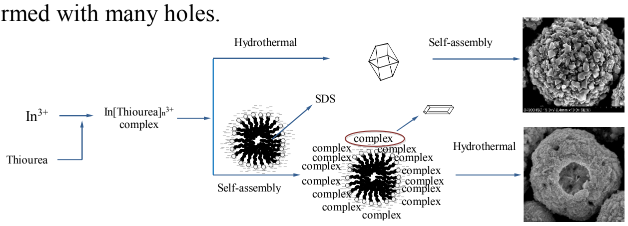

Scheme 1 Schematic drawing of the possible mechanism for the formation of In_2S_3 samples.

In order to examine the quantum confinement effect of as-prepared β-In_2S_3 samples, room temperature powder ultraviolet and visible (UV-Vis) absorption were recorded with $BaSO_4$ used as a reference. Fig. 3 showed the UV-Vis absorption of as-prepared In_2S_3 samples. The energy gap of bulk In_2S_3 is 2.2 eV with the corresponding absorption edge *ca*. 560 nm.[7] From UV characterization, $\lambda_1 = 655$ nm and $\lambda_2 = 642$ nm, which are red-shifted by almost 80~90 nm compared to the absorption edge in bulk In_2S_3. Energy gap by solid ultraviolet test could be calculated according to formula $Eg = h\nu/\lambda$, so Eg(1) = 1.89 eV, Eg(2) = 1.93 eV. The step-like characteristic of the absorption spectrum correlates well with that of the In_2S_3 nanocrystals prepared by many other researchers using organic capping media and have been explained to be due to valence-conduction band transition in In_2S_3.[23] A blue-shift by almost 100 nm of the optical absorption edge of hollow-spheres sample was observed from the UV-Vis absorption spectra. This can be attributed to the size of octahedron-like polyhedrons from solid-spheres In_2S_3 is much longer than nanorods with hexahedral shape which is hollow-sphere, because particles with large size could increase scattering of incident light.

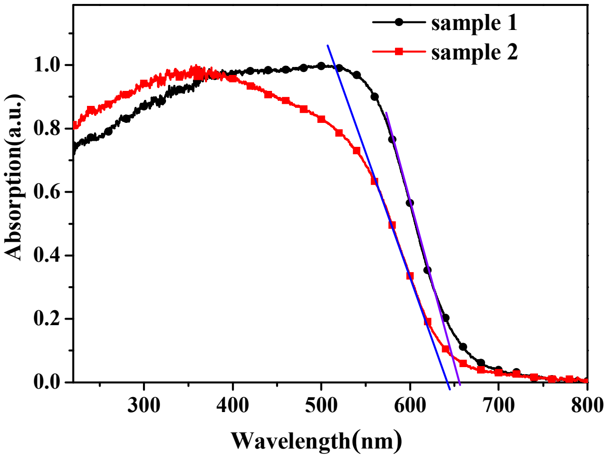

Fig. 3 UV-Vis spectra of In_2S_3 samples.

The SPV spectroscopies of the prepared In_2S_3 samples with solid-spheres and hollow-spheres structure were taken with zero bias. As characterizing In_2S_3 samples, it is assembled to be a sandwich-like consiting of indium tin oxide (ITO) glass/powder/conductor substrate and light permeate ITO electrode to effect on sample (Fig. S1). To the best of our knowledge, there are many researches studied on the optical property and electrical property of In_2S_3 crystalline material,[6] but no optoelectronic property investigation of indium sulfide by the SPV spectroscopy method has been reported yet. Fig. 4 presents the result of surface photovoltage characterization. A surface photovoltaic spectrum is a sensitive method to investigate the structural properties of the surface, surface state, the separation and recombination of the photo-carriers. Since the nanorod thickness of the hollow-spheres particle is less than 1 um, the built-in field for these particles is not as significant as that in a bulk semiconductor, in which the built-in field within the space charge region is well formed and guarantees an intense SPV response. The special hollow-spheres morphology of these microparticles is responsible for a higher contact electric resistance compared with the adjacent particles for their loose aggregation and point contact between their curved surface. This point contact blocks the charges transferring along the particles.

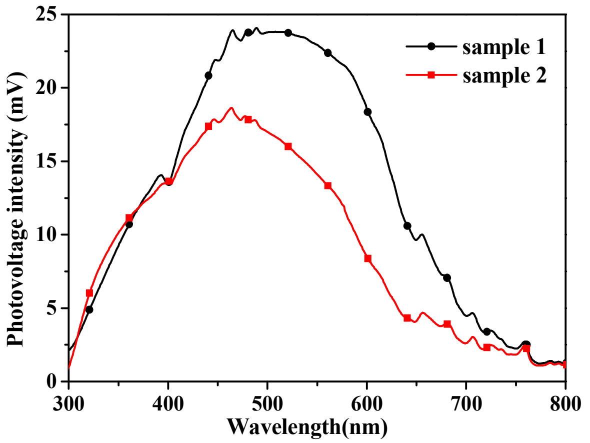

Fig. 4 SPV spectra of In_2S_3 samples

Therefore, a weak SPV response is obtained for the aggregated hollow particles. It is noticed that a strong SPV response to the light from 760 nm to 300 nm. At same photonic energy, the rod-shape may be easy to drive more electron carriers by a larger proportion in the conduction band of micro-hollow spheres to hop across the interfaces between them toward the probing electrode. Therefore, the edge of the SPV response band of sample **1** which is 688 nm, red-shifts compared to the sample **2** (676 nm), which is in well agreement with the result of UV characterization. On the other hand, maximum photovoltage of solid micro-spheres and hollow micro-spheres In_2S_3 samples come up to 23.9 mV and 18.6 mV at 465 nm and 464 nm in visible region respectively. Sample 1 showing a much higher SPV signal than sample 2 benefited from their larger average particle size. Therefore, a perfect energy band can be formed, and the photogenerated charges can be distinctly separated by the built-in field.[24] The SPV signal intensity of the as-prepared β-In_2S_3 samples can achieve millivolt level, which is stronger than other metal chalcogenides/oxides materials.[25] In fact, the pattern of SPV response maximum in the UV region is a collaborative and complicated process of energy spectral distribution of excitation light source and optical pre-absorption by the probing blank ITO electrode and the intrinsic SPV response produced in the sample.

In summary, the pure solid-spheres conposed of wedge-like octahedra and hollow-spheres composed of 1D nanorods In_2S_3 microparticles which index (JCPDS No.65-0459) were successfully synthesized by one-step hydrothermal method. Their E_g are 1.89 eV and 1.93 eV respectively. The edge of the SPV and UV response band of solid-spheres is all red-shifts compared to hollow-spheres. Maximum photovoltage of solid micro-spheres and hollow micro-spheres In_2S_3 samples come up to 23.9 mV and 18.6 mV at 465 nm and 464 nm respectively.

This work was supported by the National Natural Science Foundation of China (Grant No. 21071035 and 21171044), National key Basic Research Program of China (973 Program, No. 2013CB632900).

Notes and references

[a] *Department of Chemistry, Harbin Institute of Technology, Harbin 150001, P. R. of China. Fax: +86-451-86418270; Tel.: +86-451-86413710; E-mail address: ylyang@hit.edu.cn; fanruiqing@hit.edu.cn*

† Electronic Supplementary Information (ESI) available: Details of characterization, and the sandwich-like structure of SPV measurement. See DOI: 10.1039/b000000x/

1 (*a*) J. T. Hu, T. W. Odom and C. M. Lieber, *Acc. Chem. Res.*, 1999, **32**, 435–445; (*b*) Y. Sun and Y. Xia, *Science*, 2002, **298**, 2176–2179; (*c*) B. Nikoobakht and M. A. El-Sayed, *Chem. Mater.*, 2003, **15**,1957–1962; (*d*) J. H. Ahn, H. S. Kim, K. J. Lee, S. Jeon, S. J. Kang, Y. Sun, R. G. Nuzzo and J. A. Rogers, *Science*, 2006, **314**, 1754–1757; (*e*) J. A. Hubbell and A. Chilkoti, *Science*, 2012, **337**, 303–305; (*f*) C. Burda, X. Chen, R. Narayanan and M. A. El-Sayed, *Chem. Rev.*, 2005, **105**, 1025–1102.

2 K. F. Mak, K. He, C. Lee, G. H. Lee, J. Hone, T. F. Heinz and J. Shan, *Nature Mater.*, 2013, **13**, 207–211.

3 M. Pang, J. Hu, and H. C. Zeng, *J. Am. Chem. Soc.*, 2010 , **132** , 10771–10785.

4 K. Girija, S. Thirumalairajan, A. K. Patra, D. Mangalaraj, N. Ponpandian and C. Viswanathan, *Curr. Appl. Phys.*, 2013, **13**, 652–658.

5 X.P. Lin, D.M. Song, X.Q. Gu, Y.L. Zhao and Y.H. Qiang. *Appl. Surf. Sci.*, 2012, **263**, 816–820.

6 (*a*) K. H. Park, K. Jang, and S. U. Son, *Angew. Chem. Int. Ed.*, 2006, **45**, 4608–4612; (*b*) E. Dalas and L. Kobotiatis, *J. Mater. Sci.*, 1993, **28**, 5456–5460; (*c*) A. Datta, G. Sinha, S. K. Panda, and A. Patra, *Cryst. Growth & Des.*, 2009, **9**, 427–431; (*d*) Y. Sharma and P. Srivastava. *Mater. Chem. Phys.*, 2012, **135**, 385–394.

7 T. Asikainen, M. Ritala and M. Leskela, *Appl. Surf. Sci.*, 1994, **82/83**,122–125.

8 (*a*) T. Dittrich, D. Kieven, A. Belaidi, M. Rusu, J. Tornow, K. Schwarzburg and M. Ch. Lux-Steiner, *J. Appl. Phys.*, 2009, **105**, 034509; (*b*) M. Krunks, E. Kärber, A. Katerski, K. Otto, I. O. Acik, T. Dedova and A. Mere, *Sol. Energy Mater. Sol. Cells*, 2010, **94**, 1191–1995.

9 C. Liang, Y. Shimizu, T. Sasaki, H. Umehara and N. Koshizaki, *J. Mater. Chem.*, 2004, **14**, 248–252.

10 M. Afzaal, M. A. Malik and P. O'Brien. *Chem. Commun.*, 2004, 334–335.

11 G. D. Liu, X. L. Jiao and Z. H. Qin. *Cryst. Eng. Comm.*, 2011, **13**, 182–187.

12 (*a*) Y. Xing, H. Zhang, S. Song, J. Feng, Y. Lei, L. Zhao and M. Li, *Chem. Commun.*, 2008, 1476–1478; (*b*) G. Li and H. Liu, *J. Mater. Chem.*, 2011, **21**, 18398–18402.

13 S. Acharya, M. Dutta and S. Sarkar, *Chem. Mater.*, 2012, **24**, 1779–1785.

14 A. Datta, G. Sinha and S. K. Panda, *Cryst. Growth & Des.*, 2009, **9**, 427–431.

15 G. D. Liu, X. L. Jiao and Z. H. Qin, *Cryst. Eng. Comm.*, 2011, **13**, 182–187.

16 S. Rengaraj, S. Venkataraj, C. Tai, Y. Kim, E. Repo, and M. Sillanpää, *Langmuir*, 2011, **27**, 5534–5541.

17 H. G. Yang and H. C. Zeng, *J. Phys. Chem. B*, 2004, 108, 3492–3495; Y. Chang, J. J. Teo and H. C. Zeng, *Langmuir*, 2005, **21**, 1074–1079.

18 N. -G. Park, M. G. Kang, K. S. Ryu, K. M. Kim, and S. H. Chang, *J. Photochem. Photobiol. A*, 2004, **161**, 105–110.

19 F. Cao, W. Shi, R. Deng, S. Song, Y. Lei, S. Wang and S. Su, *Solid State Sci.*, 2010, **12**, 39–44.

20 J. Q. Hu, B. Deng, W. X. Zhang, K. B. Tang and Y. T. Qian, *Inorg. Chem.*, 2001, **40**, 3130–3133.

21 L. Zhang, W. Zhang, H. Yang, W. Fu, M. Li, H. Zhao and J. Ma, *Appl. Surf. Sci.*, 2012, **258**, 9018–9024; J. Yang, C. Lin, Z. Wang and J. Lin, *Inorg. Chem.*, 2006, **45**, 8973–8979; B. Li, Y. Xie and Y. Xue, *J. Phys. Chem. C*, 2007, **111**, 12181–12187.

22 (*a*) X. Wu and C. M. Crudden, *Chem. Mater.*, 2012, **24**, 3839–3846; (*b*) Y. Xiong, Y. Xie, J. Yang, R. Zhang, C. Wu and G. Du, *J. Mater. Chem.*, 2002, **12**, 3712–3716.

23 (*a*) A. Datta, D. Mukherjee, S. Witanachchi and P. Mukherjee, *RSC Adv.*, 2013, **3**, 141–147; (*b*) W. Chen, J. O. Bovin, A. G. Joly, S. Wang, F. Su and G. Li, *J. Phys. Chem. B*, 2004, **108**, 11927–11934; (*c*) K. H. Park, K. Jang and S. U. Son, *Angew. Chem. Int. Ed.*, 2006, **45**, 4608–4612.

24 Y. Lin, D. Wang, Q. Zhao, M. Yang and Q. Zhang, *J. Phys. Chem. B*, 2004, **108**, 3202–3206.

25 (*a*) H. Li, Q. Zhao, X. Li, Y. Shi and G. Chen, *Appl. Surf. Sci.*, 2012, **258**, 7099–7104; (*b*) D. Wang, Y. Cao, X. Zhang, Z. Liu and X. Qian, *Chem. Mater.*, 1999, **11**, 392–398.